

Microscopic $NN \rightarrow NN^*(1440)$ transition potential: Determination of $\pi NN^*(1440)$ and $\sigma NN^*(1440)$ coupling constants

B. Juliá-Díaz,¹ A. Valcarce,^{1,2} P. González,² and F. Fernández¹

¹*Grupo de Física Nuclear, Universidad de Salamanca, E-37008 Salamanca, Spain*

²*Departamento de Física Teórica and IFIC, Universidad de Valencia - CSIC, E-46100 Burjassot, Valencia, Spain*

(Received 21 January 2002; published 26 August 2002)

A $NN \rightarrow NN^*(1440)$ transition potential, based on an effective quark-quark interaction and a constituent quark cluster model for baryons, is derived in the Born-Oppenheimer approach. The potential shows significant differences with respect to those obtained by a direct scaling of the nucleon-nucleon interaction. From its asymptotic behavior we extract the values of $\pi NN^*(1440)$ and $\sigma NN^*(1440)$ coupling constants in a particular coupling scheme.

DOI: 10.1103/PhysRevC.66.024005

PACS number(s): 12.39.Jh, 13.75.Cs, 14.20.Gk, 24.85.+p

I. INTRODUCTION

The nucleon-nucleon (NN) interaction constitutes the basic process in nuclear dynamics and as such it has been for many years the object of extensive study. Different approaches, going from almost completely phenomenological potentials and meson-exchange treatments at the baryon level to quark model descriptions, have been developed to mitigate the current impossibility to directly obtain the form of the interaction from QCD. Each approach has its own justification. The use of more and more sophisticated phenomenological baryonic potentials allows a very precise fit of some data in a selected energy domain. Meson-exchange approaches at the baryon level make clear the role of effective hadronic degrees of freedom at a given energy scale. Quark model descriptions based on QCD and formulated in terms of effective quark degrees of freedom might be the closest approach to the underlying theory.

From all of them we have been able to reach a quite reasonable, though not complete, understanding of the two-nucleon interaction at low energy ($T_{\text{lab}} \leq 300$ MeV) [1–5]. When increasing the energy, the opening of channels involving the excitation of baryon resonances determines to a good extent the character of the interaction. Up to 1 GeV relative kinetic energy in the laboratory, the $\Delta(1232)$ and $N^*(1440)$ are the most prominent resonances [6]. The role played by the Δ resonance has been studied at the baryon level [7–15] as well as at the quark level [16–18], by means of $NN \rightarrow N\Delta$, $N\Delta \rightarrow N\Delta$, and $\Delta\Delta \rightarrow \Delta\Delta$ potentials. These studies show the relevance of a quark analysis to properly treat the short-range part of the interaction.

The $N^*(1440)$ (Roper) is a broad resonance which couples strongly (60–70 %) to the πN channel and significantly (5–10 %) to the σN channel [19]. These features suggest that the Roper resonance should play an important role in nuclear dynamics as an intermediate state. This role has been analyzed at the baryon level. Graphs involving the excitation of $N^*(1440)$ appear in different systems, as for example the neutral pion production in proton-proton reactions [20] or the three-nucleon interaction mediated by π and σ exchange contributing to the triton binding energy [21]. The excitation of the Roper resonance has also been used to ex-

plain the missing energy spectra in the $p(\alpha, \alpha')$ reaction [22] or the $np \rightarrow d(\pi\pi)^0$ reaction [23]. The coupling of the $N^*(1440)$ to πN and σN channels could also be important in heavy ion collisions at relativistic energies [24,25]. The presence of $NN^*(1440)$ configurations on the deuteron has been suggested long ago [26–29]. Finally, pion electroproduction and photoproduction may take place through the $N^*(1440)$ excitation [30]. However the use of a $NN \rightarrow NN^*(1440)$ transition potential as a straightforward generalization of some pieces of the $NN \rightarrow NN$ potential plus the incorporation of resonance width effects may have, as commented above for the Δ , serious shortcomings specially concerning the short-range part of the interaction [16–18,31].

In view of the current interest in nucleon resonances in a nuclear physics context, it seems appropriate to extend the quark model NN calculations to treat all presently accepted N^* resonances. In this article we propose a quark model treatment of the $NN \rightarrow NN^*(1440)$ interaction. We shall adopt the same quark model approach previously used for the Δ case and also applied to the $NN^*(1440) \rightarrow NN^*(1440)$ interaction [31]. We shall center our attention in the derivation of a $NN \rightarrow NN^*(1440)$ transition potential from a quark-quark (qq) basic interaction incorporating gluon, pion and sigma exchanges. For the sake of simplicity we shall follow a Born-Oppenheimer (BO) approximation with harmonic oscillator baryon wave functions written in terms of quarks. The Roper resonance, $N^*(1440)$, will be considered as a stable particle.

A main feature of our quark treatment is its universality in the sense that all the baryon-baryon interactions are treated on an equal footing. Moreover, once the model parameters are fixed from NN data there are no free parameters for any other case. This allows a microscopic understanding and connection of the different baryon-baryon interactions that is beyond the scope of any analysis based only on effective hadronic degrees of freedom. This is important not only in the short-range regime, where it does not exist a definite prescription for the potentials at the baryon level when resonances are involved, but at all distances. In particular, the asymptotic (long-range) behavior of the $NN \rightarrow NN^*(1440)$ potential allows the determination of the $\pi NN^*(1440)$ and $\sigma NN^*(1440)$ coupling constants as well as their ratios to the

πNN and σNN coupling constants, respectively. These studies are instructive inasmuch as they are expected to lead to a deeper understanding of the nuclear potential and entail a rethinking of basic nuclear concepts from the point of view of the fundamental quark substructure.

The article is organized as follows. In Sec. II we write the qq interaction and analyze the two-baryon wave functions in order to obtain the $NN \rightarrow NN^*(1440)$ transition potential. In Sec. III we draw the results for different partial waves and spin-isospin channels. In Sec. IV we proceed to determine the $\pi NN^*(1440)$ and $\sigma NN^*(1440)$ coupling constants and relate them to the πNN and σNN coupling constants. Finally, in Sec. V we summarize our main conclusions.

II. $NN \rightarrow NN^*(1440)$ TRANSITION POTENTIAL

In the Born-Oppenheimer approximation the $NN \rightarrow NN^*(1440)$ transition potential at the interbaryon distance R is obtained by sandwiching between NN and $NN^*(1440)$ states (expressed in terms of quarks) the qq potential for all the pairs formed by two quarks belonging to different baryons. In other words,

$$V_{NN(LST) \rightarrow NN^*(L'S'T)}(R) = \xi_{LST}^{L'S'T}(R) - \xi_{LST}^{L'S'T}(\infty), \quad (1)$$

where

$$\begin{aligned} \xi_{LST}^{L'S'T}(R) &= \frac{\left\langle \Psi_{NN^*}^{L'S'T}(\vec{R}) \left| \sum_{i < j = 1}^6 V_{qq}(\vec{r}_{ij}) \right| \Psi_{NN}^{LST}(\vec{R}) \right\rangle}{\sqrt{\langle \Psi_{NN^*}^{L'S'T}(\vec{R}) | \Psi_{NN^*}^{L'S'T}(\vec{R}) \rangle} \sqrt{\langle \Psi_{NN}^{LST}(\vec{R}) | \Psi_{NN}^{LST}(\vec{R}) \rangle}}. \end{aligned} \quad (2)$$

The quark-quark potential has been very much detailed elsewhere [4,5] and it will only be written here for completeness. It reads

$$V_{qq}(\vec{r}_{ij}) = V_{\text{con}}(\vec{r}_{ij}) + V_{\text{OGE}}(\vec{r}_{ij}) + V_{\text{OPE}}(\vec{r}_{ij}) + V_{\text{OSE}}(\vec{r}_{ij}), \quad (3)$$

where \vec{r}_{ij} is the interquark distance. V_{con} is the confining potential, whose detailed radial structure being fundamental to study the hadron spectra is expected to play a minor role for the two-baryon interaction [32]. To be consistent with baryon and meson spectroscopy it will be taken to be linear

$$V_{\text{con}}(\vec{r}_{ij}) = -a_c \vec{\lambda}_i \cdot \vec{\lambda}_j r_{ij}, \quad (4)$$

where the λ 's stand for the color SU(3) matrices. V_{OGE} is the perturbative one-gluon-exchange (OGE) interaction containing Coulomb ($1/r_{ij}$), spin-spin ($\vec{\sigma}_i \cdot \vec{\sigma}_j$), and tensor terms (S_{ij}) [33]

TABLE I. Quark-model parameters.

m_q (MeV)	313
b (fm)	0.518
α_s	0.485
α_{ch}	0.027
m_σ (fm $^{-1}$)	3.42
m_π (fm $^{-1}$)	0.70
Λ (fm $^{-1}$)	4.2

$$\begin{aligned} V_{\text{OGE}}(\vec{r}_{ij}) &= \frac{1}{4} \alpha_s \vec{\lambda}_i \cdot \vec{\lambda}_j \left\{ \frac{1}{r_{ij}} - \frac{\pi}{m_q^2} \left[1 + \frac{2}{3} \vec{\sigma}_i \cdot \vec{\sigma}_j \right] \delta(\vec{r}_{ij}) \right. \\ &\quad \left. - \frac{3}{4m_q^2 r_{ij}^3} S_{ij} \right\}, \end{aligned} \quad (5)$$

and V_{OPE} and V_{OSE} are the one-pion (OPE) and one-sigma exchange (OSE) interactions given by

$$\begin{aligned} V_{\text{OPE}}(\vec{r}_{ij}) &= \frac{1}{3} \alpha_{ch} \frac{\Lambda^2}{\Lambda^2 - m_\pi^2} m_\pi \left\{ \left[Y(m_\pi r_{ij}) \right. \right. \\ &\quad \left. \left. - \frac{\Lambda^3}{m_\pi^3} Y(\Lambda r_{ij}) \right] \vec{\sigma}_i \cdot \vec{\sigma}_j + \left[H(m_\pi r_{ij}) \right. \right. \\ &\quad \left. \left. - \frac{\Lambda^3}{m_\pi^3} H(\Lambda r_{ij}) \right] S_{ij} \right\} \vec{\tau}_i \cdot \vec{\tau}_j, \end{aligned} \quad (6)$$

$$\begin{aligned} V_{\text{OSE}}(\vec{r}_{ij}) &= -\alpha_{ch} \frac{4m_q^2}{m_\pi^2} \frac{\Lambda^2}{\Lambda^2 - m_\sigma^2} m_\sigma \left\{ Y(m_\sigma r_{ij}) \right. \\ &\quad \left. - \frac{\Lambda}{m_\sigma} Y(\Lambda r_{ij}) \right\}, \end{aligned} \quad (7)$$

where Λ is a cutoff parameter and

$$Y(x) = \frac{e^{-x}}{x}, \quad (8)$$

$$H(x) = \left(1 + \frac{3}{x} + \frac{3}{x^2} \right) Y(x). \quad (9)$$

The values chosen for the parameters are tabulated in Table I. They are taken from Ref. [5] where an accurate description of the NN scattering phase shifts and the deuteron properties is obtained. They also provide a reasonable description of the baryon spectrum [34].

The Born-Oppenheimer approximation followed integrates out the quark coordinates keeping R fixed. Hence, quantum fluctuations of the two-baryon center-of-mass are neglected. Nonetheless, a more complete treatment as the one implied by the use of the resonating group method may not represent, at least for the calculations we perform, major changes as it turns out to be the case for the NN interaction [35].

The NN and $NN^*(1440)$ wave functions we shall use hereforth have been also detailed elsewhere [31]. Here we only quote some results that will be useful in what follows. The N and $N^*(1440)$ states are given in terms of quarks by

$$|N\rangle = |[3](0s)^3] \otimes [1^3]_c, \quad (10)$$

$$|N^*(1440)\rangle = \left\{ \sqrt{\frac{2}{3}} |[3](0s)^2(1s)] - \sqrt{\frac{1}{3}} |[3](0s)(0p)^2] \right\} \otimes [1^3]_c, \quad (11)$$

where $[1^3]_c$ is the completely antisymmetric color state, $[3]$ is the completely symmetric spin-isospin state and $0s$, $1s$, and $0p$, stand for harmonic oscillator orbitals.

For a definite orbital angular momentum L and spin S , the NN wave function satisfies, due to the identity of the baryons, the selection rule

$$L_{NN} - S_{NN} - T_{NN} = \text{odd}. \quad (12)$$

This is not the case for the $NN^*(1440)$ system, due to the nonidentity of N and $N^*(1440)$. Nevertheless antisymmetry at quark level, coming from the identity of quarks, gives rise to a generalized selection rule for any nucleon resonance N^* , that can be written as

$$L_{NN^*} - S_{NN^*} - T_{NN^*} + f = \text{odd}, \quad (13)$$

where f is the NN^* spin-isospin parity determining the symmetric ($f = \text{even}$) or antisymmetric ($f = \text{odd}$) character of the NN^* wave function in the spin-isospin space. The case $f = \text{even}$ gives rise to the same NN^* channels than in the NN case, whereas the case $f = \text{odd}$ corresponds to channels forbidden in the NN case that reflects the effects of quark identity beyond baryon identity. These *forbidden* channels play a relevant role in the $NN^*(1440) \rightarrow NN^*(1440)$ case [31]. However for the $NN \rightarrow NN^*(1440)$ transition we are dealing with the situation simplifies considerably. In fact, as the strong interaction preserves isospin we have $T_{NN^*} = T_{NN}$. Furthermore the structure of the interaction given by Eq. (3) allows only to connect NN and $NN^*(1440)$ channels verifying $L' - L = 0$ or $2 = S' - S$. Therefore the initial state selection rule translates to the final state, i.e., only $f = \text{even}$ $NN^*(1440)$ channels are allowed.

The most representative diagrams contributing to the $NN \rightarrow NN^*(1440)$ potential, as calculated from Eq. (1), are drawn in Fig. 1. We distinguish between the direct diagrams (labeled as V_{36} in Fig. 1), not involving quark exchanges, and the rest of diagrams including exchange of quarks (labeled as $V_{ij}P_{36}$ in Fig. 1). Most diagrams contributing to the interaction are due to the first term of the $N^*(1440)$ wave function ($|[3](0s)^2(1s)]$), only a few of them, those with two vertical dashed lines, correspond to the second term of the $N^*(1440)$ wave function ($|[3](0s)(0p)^2]$).

III. RESULTS

In Figs. 2, 3, and 4, we show the potentials obtained for $L=0$ (1S_0 and 3S_1), $L=1$ (1P_1 and 3P_0), and $L=2$ (1D_2

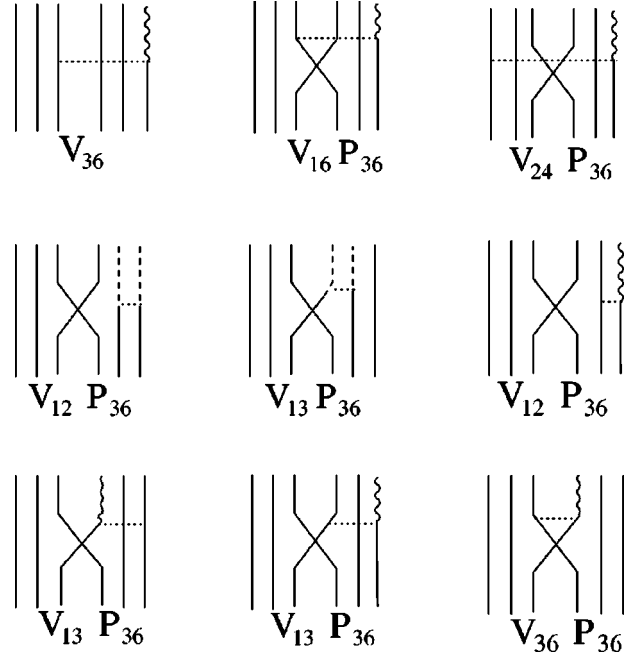


FIG. 1. Different diagrams contributing to the $NN \rightarrow NN^*(1440)$ interaction. The wavy line denotes an excited quark on the $1s$ shell and the dashed line stands for an excited quark on the $0p$ shell. We have labeled the diagrams attending to their topological equivalence, although they involve interactions between excited or nonexcited quarks. This simplified notation will be used in the next figures to separate the different contributions to the interaction.

and 3D_1) partial waves, respectively. Contributions from the different terms of the potential as separated in Eq. (3) have been made explicit. For some selected partial waves, we separate in Fig. 5 the contribution of the different diagrams depicted in Fig. 1. Let us mention that an arbitrary global phase between the N and $N^*(1440)$ wave functions as written in Eqs. (10) and (11) has to be chosen. We will discuss all aspects depending on this choice.

There are a number of general features that can be enumerated.

(i) The very long-range part of the interaction ($R > 4$ fm) comes dominated, as for the $NN \rightarrow NN$ and $NN^*(1440) \rightarrow NN^*(1440)$ cases, by the one-pion exchange, the longest-range piece of the potential. However the asymptotic potential reverses sign with respect to both $NN \rightarrow NN$ and $NN^*(1440) \rightarrow NN^*(1440)$. Thus for S and D waves the $NN \rightarrow NN^*(1440)$ interaction is asymptotically repulsive. This sign reversal is a direct consequence of the presence of a node in the $N^*(1440)$ wave function what implies a change of sign with respect to the N wave function at long distances [if the opposite sign for the $N^*(1440)$ wave function were chosen the very long-range part of the interaction would be attractive but there would also be a change in the character of the short-range part]. This is also corroborated by the study of the one-sigma exchange interaction that is always asymptotically repulsive at difference to the $NN \rightarrow NN$ and $NN^*(1440) \rightarrow NN^*(1440)$ cases [for

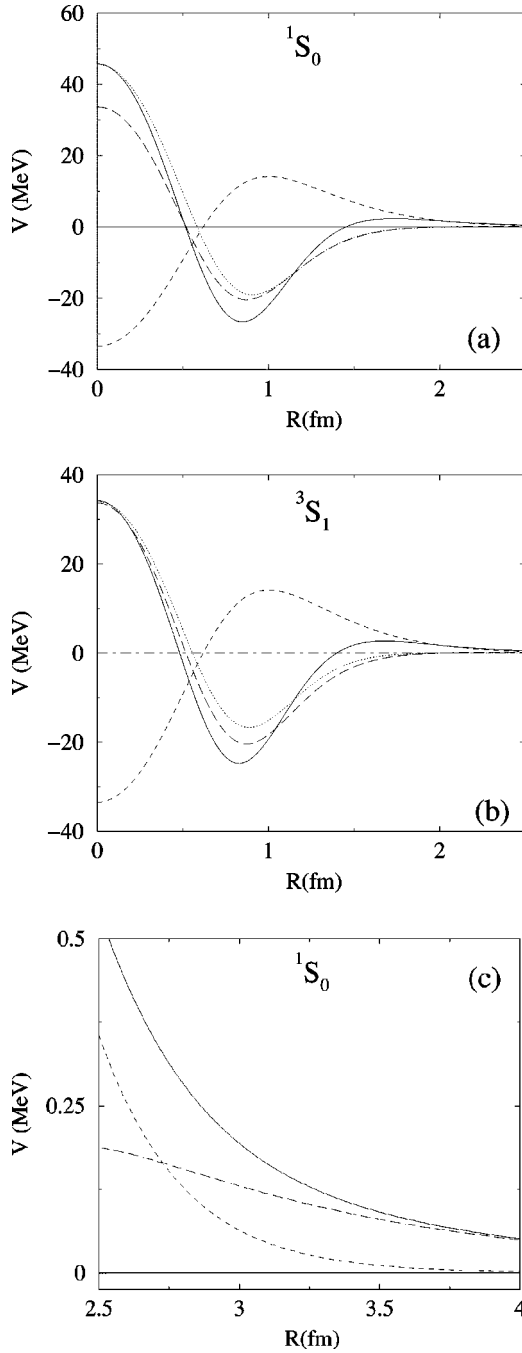


FIG. 2. $NN \rightarrow NN^*(1440)$ potential for (a) the 1S_0 partial wave, (b) the 3S_1 partial wave, and (c) the long-range part of the 1S_0 partial wave. We have denoted by the long-dashed, dashed, dotted, and dot-dashed lines, the central OPE, OSE, OGE, and the tensor contributions, respectively. By the solid line we plot the total potential.

$NN^*(1440) \rightarrow NN^*(1440)$ there are two compensating changes of sign coming from the two Ropers].

It is worth to remark that no quark antisymmetrization effects survive either in the numerator or in the denominator (norm) of Eq. (1) at these distances. In other words, the potential corresponds to a direct baryon-baryon interaction.

(ii) For the long-range $2 < R < 4$ fm part, the one-pion and one-sigma-exchange potentials altogether determine the

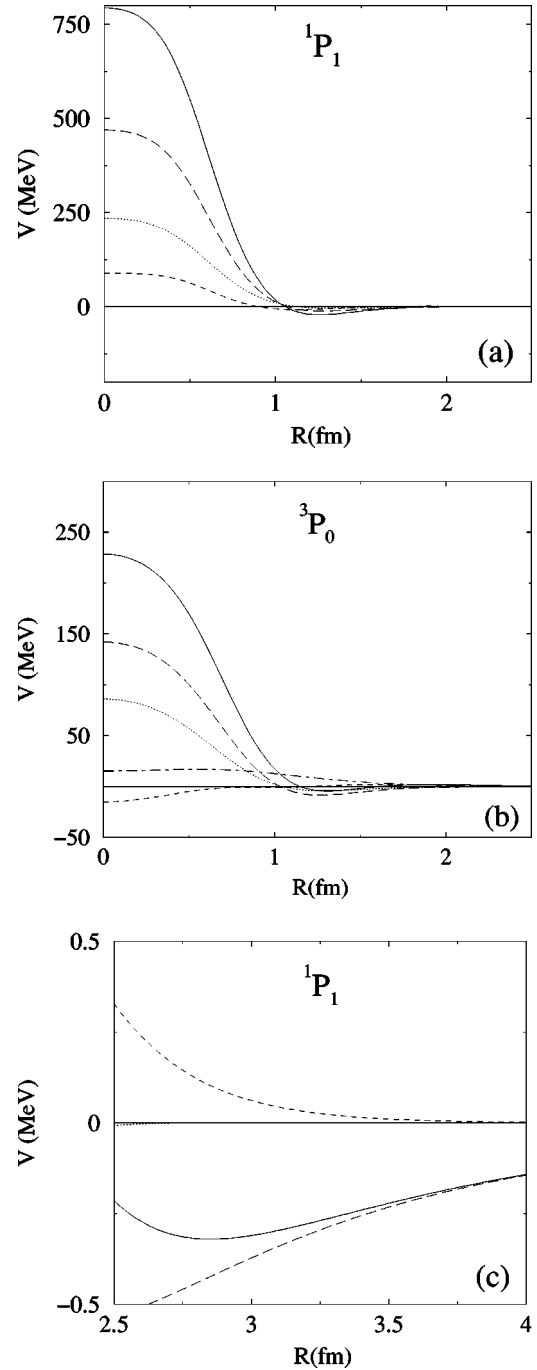


FIG. 3. Same as Fig. 2 but for (a) the 1P_1 partial wave, (b) the 3P_0 partial wave, and (c) the long-range part of the 1P_1 partial wave.

character of the interaction, since the one-gluon exchange gives a negligible contribution for $R \geq 2$ fm. One should also notice that although the contribution from quark exchange diagrams is very much suppressed for $R \geq 2$ fm, some quark antisymmetrization effects may still be present through the norm (see Fig. 1 of Ref. [31]).

(iii) At intermediate range $0.6 < R < 2$ fm a complex interplay among all pieces of the potential (gluon, pion, and sigma) generates the final form of the interaction. When decreasing R from 2 fm to 0.6 fm two effects take place. On the

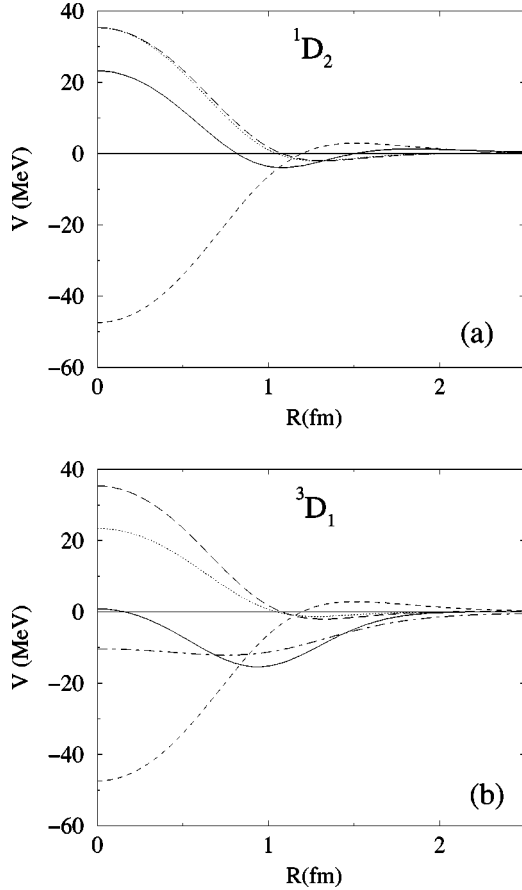


FIG. 4. Same as Fig. 2 but for (a) the 1D_2 partial wave and (b) the 3D_1 partial wave.

one hand, quark exchange diagrams are increasingly important becoming dominant below $R=1.5$ fm. On the other hand the different pieces of the potential are changing sign: from attractive to repulsive for the gluon in all partial waves, from repulsion to attraction for the sigma in S and D waves and from repulsion to attraction and again to repulsion for the pion in S and D waves. As a combined result of these effects the total potential turns out to be attractive from $R=1.5$ fm down to a lower value of R different for each partial wave. This behavior, related again to the node in the Roper wave function, contrasts with the $NN \rightarrow NN$ and $NN^*(1440) \rightarrow NN^*(1440)$ cases, where for instance for S and D waves the scalar (sigma) part keeps always the same sign and gives the dominant contribution for $R > 0.8$ fm.

(iv) The choice of 0.6 fm as a lower limit for the intermediate range comes motivated by the repulsive character of the potential in all partial waves for shorter distances. The one-gluon and one-pion quark exchange parts are mainly responsible for such a repulsion as it turns out to be the case for $NN \rightarrow NN$ and $NN^*(1440) \rightarrow NN^*(1440)$. Nevertheless there are two distinctive features with respect to these cases: in $NN \rightarrow NN^*(1440)$ the intensity of the repulsion at $R=0$ and the value of R at which the interaction becomes repulsive are significantly lower than in $NN \rightarrow NN$ and $NN^*(1440) \rightarrow NN^*(1440)$. This is a clear effect of the more

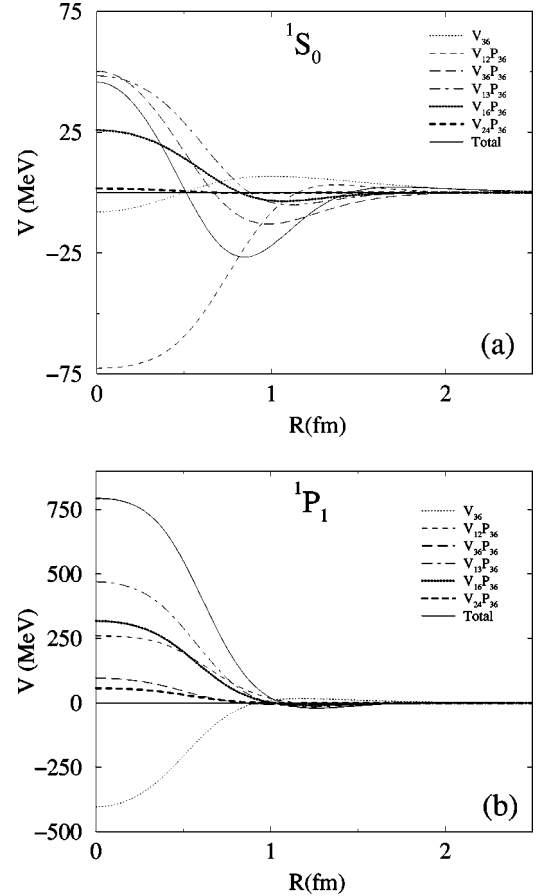


FIG. 5. $NN \rightarrow NN^*(1440)$ potential for (a) the 1S_0 partial wave and (b) the 1P_1 partial wave. We have made explicit the contribution of the different diagrams shown in Fig. 1, with the convention explained in the caption.

similarity (higher overlap) in these cases between initial and final states what makes the Pauli principle more active.

IV. $\pi NN^*(1440)$ AND $\sigma NN^*(1440)$ COUPLING CONSTANTS

The potential obtained can be also written at all distances in terms of baryonic degrees of freedom [36]. One should realize that a qq spin and isospin independent potential as for instance the scalar one-sigma exchange, gives rise at the baryon level, apart from a spin-isospin independent potential, to a spin-spin, an isospin-isospin and a spin-isospin dependent interaction [4]. Nonetheless for distances $R \geq 4$ fm, where quark antisymmetrization interbaryon effects vanish, we are only left with the direct part, i.e., with a scalar one-sigma exchange at the baryon level. The same kind of argument can be applied to the one-pion exchange potential. Thus asymptotically ($R \geq 4$ fm) OSE and OPE have at the baryon level the same spin-isospin structure than OSE and OPE at the quark level. Hence we can parametrize the asymptotic central interactions as (the Λ depending exponential term is negligible asymptotically as compared to the Yukawa term)

$$\begin{aligned}
 V_{NN \rightarrow NN^*(1440)}^{\text{OPE}}(R) &= \frac{1}{3} \frac{g_{\pi NN}}{\sqrt{4\pi}} \frac{g_{\pi NN^*(1440)}}{\sqrt{4\pi}} \frac{m_\pi}{2M_N} \frac{m_\pi}{2(2M_r)} \\
 &\times \frac{\Lambda^2}{\Lambda^2 - m_\pi^2} [(\vec{\sigma}_N \cdot \vec{\sigma}_N)(\vec{\tau}_N \cdot \vec{\tau}_N)] \frac{e^{-m_\pi R}}{R}
 \end{aligned} \quad (14)$$

and

$$V_{NN \rightarrow NN^*(1440)}^{\text{OSE}}(R) = -\frac{g_{\sigma NN}}{\sqrt{4\pi}} \frac{g_{\sigma NN^*(1440)}}{\sqrt{4\pi}} \frac{\Lambda^2}{\Lambda^2 - m_\sigma^2} \frac{e^{-m_\sigma R}}{R}, \quad (15)$$

where g_i stands for the coupling constants at the baryon level and M_r is the reduced mass of the $NN^*(1440)$ system [$1/M_r = 1/M_N + 1/M_{N^*(1440)}$]. One should note that at these distances the use of the BO approximation is justified and the resonating group method potential would give quite the same results.

By comparing these baryonic potentials with the asymptotic behavior of the OPE and OSE previously obtained from the quark calculation we can extract the $\pi NN^*(1440)$ and $\sigma NN^*(1440)$ coupling constants. As the parameters at the quark level are fixed once for all from the NN interaction our results allow a prediction of these constants in terms of the elementary πqq coupling constant and the one-baryon model dependent structure. The sign obtained for the meson- $NN^*(1440)$ coupling constants and for their ratios to the meson- NN coupling constants is ambiguous since it comes determined by the arbitrarily chosen relative sign between the N and $N^*(1440)$ wave functions. Only the ratios between the $\pi NN^*(1440)$ and $\sigma NN^*(1440)$ would be free of this uncertainty. This is why we will quote absolute values except for these cases where the sign is a clear prediction of the model. To get such a prediction we can use any partial wave. We shall use for simplicity the 1S_0 wave, this is why we only wrote the central interaction in Eq. (14).

The $\Lambda^2/(\Lambda^2 - m_i^2)$ vertex factor comes from the vertex form factor chosen at momentum space as a square root of monopole [$\Lambda^2/(\Lambda^2 + \vec{q}^2)$] $^{1/2}$, the same choice taken at the quark level, where chiral symmetry requires the same form for pion and sigma. A different choice for the form factor at the baryon level, regarding its functional form as well as the value of Λ , would give rise to a different vertex factor and eventually to a different functional form for the asymptotic behavior. For instance, for a modified monopole form [$(\Lambda^2 - m^2)/(\Lambda^2 - q^2)$] $^{1/2}$, where m is the meson mass (m_π or m_σ), the vertex factor would be 1, i.e., $(\Lambda^2 - m^2)/(\Lambda^2 - m^2)$, keeping the potential the same exponentially decreasing asymptotic form. Then it is clear that the extraction from any model of the meson-baryon-baryon coupling constants depends on this choice. We shall say they depend on the coupling scheme.

For the one-pion exchange and for our value of $\Lambda = 4.2 \text{ fm}^{-1}$, $\Lambda^2/(\Lambda^2 - m_\pi^2) = 1.03$, pretty close to 1. As a consequence, in this case the use of our form factor or the modified monopole form at baryonic level makes little dif-

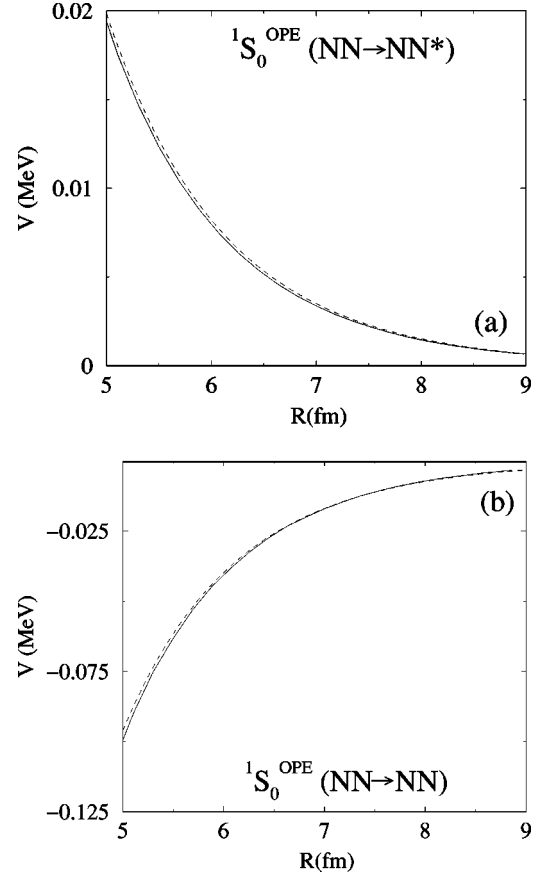


FIG. 6. (a) Asymptotic behavior of the one-pion exchange 1S_0 $NN \rightarrow NN^*(1440)$ potential (solid line). The dashed line denotes the fitted curve according to Eq. (14). (b) Same as (a) but for the one-pion exchange 1S_0 $NN \rightarrow NN$ potential.

ference in the determination of the coupling constant. This fact is used when fixing $g_{\pi qq}^2/4\pi$ from the experimental value of $g_{\pi NN}^2/4\pi$ extracted from NN data. The value we use for

$$\begin{aligned}
 \alpha_{ch} &= (m_\pi^2/4m_q^2)(g_{\pi qq}^2/4\pi) \\
 &= (\frac{3}{5})^2 (g_{\pi NN}^2/4\pi)(m_\pi^2/4m_N^2) e^{-m_\pi^2 b^2/2} = 0.027
 \end{aligned}$$

corresponds to $g_{\pi NN}^2/4\pi = 14.83$.

To get $g_{\pi NN^*(1440)}/\sqrt{4\pi}$ we turn to our numerical results for the 1S_0 OPE potential, Fig. 6(a), and fit its asymptotic behavior (in the range $R: 5 \rightarrow 9 \text{ fm}$) to Eq. (14). We obtain

$$\frac{g_{\pi NN}}{\sqrt{4\pi}} \frac{g_{\pi NN^*(1440)}}{\sqrt{4\pi}} \frac{\Lambda^2}{\Lambda^2 - m_\pi^2} = -3.73, \quad (16)$$

i.e., $g_{\pi NN^*(1440)}/\sqrt{4\pi} = -0.94$. As explained above only the absolute value of this coupling constant is well defined. Let us note that in Ref. [37] a different sign with respect to our coupling constant is obtained what is a direct consequence of the different global sign chosen for the $N^*(1440)$ wave function. The coupling scheme dependence can be explicitly eliminated if we compare $g_{\pi NN^*(1440)}$ with $g_{\pi NN}$ extracted from the $NN \rightarrow NN$ potential within the same quark model approximation, Fig. 6(b). Thus we get

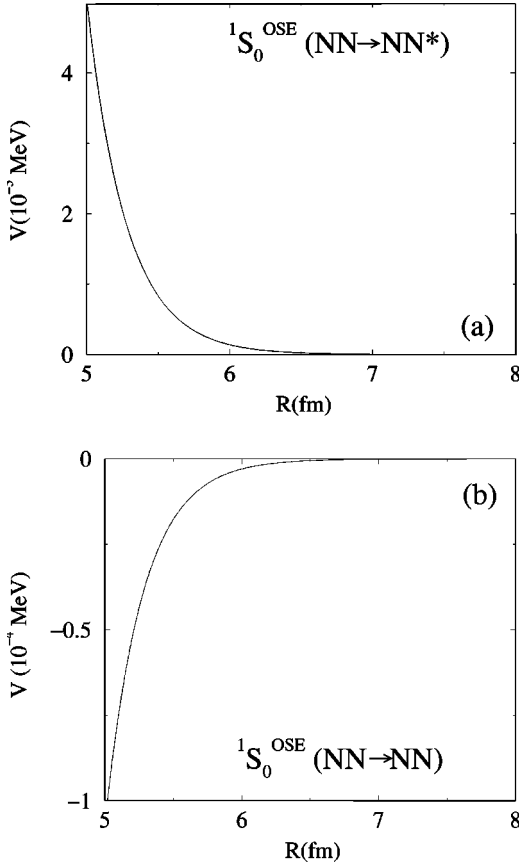


FIG. 7. (a) Asymptotic behavior of the one-sigma exchange 1S_0 $NN \rightarrow NN^*(1440)$ potential (solid line). The dashed line denotes the fitted curve according to Eq. (15). (b) Same as (a) but for the one-sigma exchange 1S_0 $NN \rightarrow NN$ potential.

$$\left| \frac{g_{\pi NN^*(1440)}}{g_{\pi NN}} \right| = 0.25. \quad (17)$$

By proceeding in the same way for the OSE potential, i.e., by fitting the potential given in Fig. 7(a) to Eq. (15), and following an analogous procedure for the NN case, Fig. 7 (b), we can write

$$\left| \frac{g_{\sigma NN^*(1440)}}{g_{\sigma NN}} \right| = 0.47. \quad (18)$$

The relative phase chosen for the $N^*(1440)$ wave function with respect to the N wave function is not experimentally relevant in any two step process comprising $N^*(1440)$ production and its subsequent decay. However it will play a relevant role in those reactions where the same field (π or σ) couples simultaneously to both systems, NN and $NN^*(1440)$. In these cases the interference term between both diagrams would determine the magnitude of the cross section [22].

The ratio given in Eq. (17) is similar to that obtained in Ref. [37] and a factor 1.5 smaller than the one obtained from the analysis of the partial decay width [37]. Nonetheless one can find in the literature values for $f_{\pi NN^*(1440)}$ ranging be-

tween 0.27–0.47 coming from different experimental analyses with uncertainties associated to the fitting of parameters [23,25,30].

Regarding the ratio obtained in Eq. (18), our result agrees quite well with the only experimental available result, obtained in Ref. [22] from the fit of the cross section of the isoscalar Roper excitation in $p(\alpha, \alpha')$ in the 10–15 GeV region, where a value of 0.48 is given. Furthermore, we can give a very definitive prediction of the magnitude and sign of the ratio of the two ratios

$$\frac{g_{\pi NN^*(1440)}}{g_{\pi NN}} = 0.53 \frac{g_{\sigma NN^*(1440)}}{g_{\sigma NN}}, \quad (19)$$

which is an exportable prediction of our model.

For the sake of completeness we give the values of $g_{\sigma NN^*(1440)}$ and $g_{\sigma NN}$, though one should realize that the corresponding form factor $\Lambda^2/(\Lambda^2 - m_\sigma^2) = 2.97$ differs quite much from 1. Moreover, the quark model dependence is quite strong what can make nonsense any comparison to other values obtained in the literature within a different framework. We get

$$\frac{g_{\sigma NN}^2}{4\pi} \frac{\Lambda^2}{\Lambda^2 - m_\sigma^2} = 72.4, \quad (20)$$

i.e., $g_{\sigma NN}^2/4\pi = 24.4$, and

$$\frac{g_{\sigma NN} g_{\sigma NN^*(1440)}}{\sqrt{4\pi}} \frac{\Lambda^2}{\Lambda^2 - m_\sigma^2} = 34.3, \quad (21)$$

i.e., $g_{\sigma NN^*(1440)}^2/4\pi = 5.5$.

Concerning the absolute value of $g_{\sigma NN^*}$ some caveats are in order. Our value is scheme and quark-model dependent and should only be sensibly compared with a value obtained in the same framework. As a matter of fact, if we had extracted the quark model factor dependence from the coupling constant ($e^{m_\sigma^2 b^2/2}$) [39] the result would have been $g_{\sigma NN^*(1440)}^2/4\pi = 1.14$ that compares quite well with the value given in Ref. [22], $g_{\sigma NN^*(1440)}^2/4\pi = 1.33$. With respect to the results given in Ref. [38] they are very sensitive to both the decay width of the sigma meson into two pions and the mass of the sigma as reflected in the large error bars given. Both quantities are highly undetermined in the Particle Data Book [19], the mass of the sigma being constrained between 400–1200 MeV and the width between 600–1000 MeV. These values have been fixed arbitrarily in Ref. [38] to $m_\sigma = 500$ MeV and $\Gamma_\sigma = 250$ MeV. Varying the mass of the sigma between 400 and 700 MeV for a fixed width of 250 MeV, the coupling constant according to Eq. (9) of Ref. [38] varies between 0.18–2.54. Taking a width of 450 MeV the resulting coupling is 0.27–1.64. In both cases, our value lies in the interval given above what makes it compatible with the $N^*(1440)$ decay and production phenomenology.

Let us finally mention that at short distances, the interaction could be fitted in terms of two different Yukawa func-

tions, one depending on the meson mass, m , the other with a shorter range depending on $\sqrt{(M_{N(1440)} - M_{N^*(1440)} + m)m}$. These two Yukawa functions could be associated to the two diagrams with different intermediate states [mNN and $mNN^*(1440)$] appearing in time ordered perturbation theory when an effective calculation at the baryonic level is carried out [let us realize that in a quark calculation the intermediate state is always mqq , the $N - N^*(1440)$ mass difference being taken into account through the N and $N^*(1440)$ wave functions]. For practical purposes, as done in previous works [40], separable expansions of the quark-based interactions can be performed and used in standard few-body calculations.

V. SUMMARY

Starting from a quark-quark chiral symmetric interaction model and assuming simple harmonic wave functions for N and $N^*(1440)$ in terms of quarks we have derived a transition $NN \rightarrow NN^*(1440)$ potential in an adiabatic approach. The Roper resonance has been taken as a stable particle. Our results for S , P , and D waves show significant differences concerning the character of the interaction (attractive or repulsive) at intermediate and longer distances with respect to the $NN \rightarrow NN$ and $NN^*(1440) \rightarrow NN^*(1440)$ cases for the chosen $N^*(1440)$ overall phase. This has to do with the presence of a node in the Roper wave function. On the contrary the short-range interaction has the same character in all cases but the intensity gets reduced in the $NN \rightarrow NN^*(1440)$ transition as a consequence of the lesser similarity between initial and final states that makes the Pauli principle to be less active. These results show that the usual procedure of obtaining NN^* interactions by a simple scaling of the NN one should be handled with care.

The analysis of the asymptotic behavior of the potentials allows to determine the $\pi NN^*(1440)$ and $\sigma NN^*(1440)$ coupling constants on the same foot than πNN and σNN couplings. Ratios between coupling constants of the type $g_{\pi NN^*(1440)}/g_{\pi NN}$ and $g_{\sigma NN^*(1440)}/g_{\sigma NN}$ are obtained. These ratios, whose sign is ambiguous, are coupling scheme independent and they have a softened quark model dependence (when compared to the dependence of the value of each constant separately). Furthermore the model allows the prediction of not only the magnitude but also the relative sign between the two ratios.

We should finally notice that for dynamical applications our results should be implemented by the inclusion of the $N^*(1440)$ width. Quantum fluctuations of the two baryon center-of-mass, neglected here, could also play some role. Though these improvements will have a quantitative effect we do not think our predictions will be very much modified at a qualitative level. In this sense they could serve either as a first step for more refined calculations or as a possible guide for phenomenological applications.

ACKNOWLEDGMENTS

We would like to thank E. Oset for a careful reading of the manuscript and useful comments and discussion. B.J. thanks Ministerio de Ciencia y Tecnología for financial support. A.V. thanks Ministerio de Educación, Cultura y Deporte of Spain for financial support through the Salvador de Madariaga program. This work was partially funded by Dirección General de Investigación Científica y Técnica (DGI-CYT) under Contract No. BFM2001-3563, by Junta de Castilla y León under Contract No. SA-109/01, and by EC-RTN, Network ESOP, Contract No. HPRN-CT-2000-00130.

-
- [1] M. Lacombe, B. Loiseau, J.M. Richard, R. Vinh Mau, J. Côté, P. Pirès, and R. de Tourreil, Phys. Rev. C **21**, 861 (1980).
 - [2] R. Machleidt, K. Holinde, and C. Elster, Phys. Rep. **149**, 1 (1987).
 - [3] V.G.J. Stoks, R.A.M. Klomp, C.P.F. Terheggen, and J.J. de Swart, Phys. Rev. C **49**, 2950 (1994).
 - [4] F. Fernández, A. Valcarce, U. Straub, and A. Faessler, J. Phys. G **19**, 2013 (1993); A. Valcarce, A. Faessler, and F. Fernández, Phys. Lett. B **345**, 367 (1995).
 - [5] D.R. Entem, F. Fernández, and A. Valcarce, Phys. Rev. C **62**, 034002 (2000).
 - [6] H.J. Weber and H. Arenhövel, Phys. Rep. **36**, 277 (1978).
 - [7] H. Sugawara and F. von Hippel, Phys. Rev. **172**, 1764 (1968).
 - [8] H. Arenhövel, Nucl. Phys. **A247**, 473 (1975).
 - [9] A.M. Green, Rep. Prog. Phys. **39**, 1109 (1976).
 - [10] K. Holinde and R. Machleidt, Nucl. Phys. **A280**, 429 (1977).
 - [11] Lomon, Phys. Rev. D **26**, 576 (1982); P. González and E. Lomon, *ibid.* **34**, 1351 (1986).
 - [12] T.-S.H. Lee, Phys. Rev. Lett. **50**, 1571 (1983); Phys. Rev. C **29**, 195 (1984); T.-S.H. Lee and A. Matsuyama, *ibid.* **36**, 1459 (1987).
 - [13] R.B. Wiringa, R.A. Smith, and T.L. Ainsworth, Phys. Rev. C **29**, 1207 (1984).
 - [14] M.T. Peña, H. Henning, and P.U. Sauer, Phys. Rev. C **42**, 855 (1990).
 - [15] J. Haidenbauer, K. Holinde, and M.B. Johnson, Phys. Rev. C **48**, 2190 (1993).
 - [16] F. Fernández, A. Valcarce, P. González, and V. Vento, Phys. Lett. B **287**, 35 (1992); Nucl. Phys. **A567**, 741 (1994).
 - [17] A. Valcarce, F. Fernández, H. Garcilazo, M.T. Peña, and P.U. Sauer, Phys. Rev. C **49**, 1799 (1994).
 - [18] H. Garcilazo, F. Fernández, A. Valcarce, and R.D. Mota, Phys. Rev. C **56**, 84 (1997).
 - [19] Particle Data Group, D.E. Groom *et al.*, Eur. Phys. J. C **15**, 1 (2000).
 - [20] M.T. Peña, D.O. Riska, and A. Stadler, Phys. Rev. C **60**, 045201 (1999).
 - [21] S.A. Coon, M.T. Peña, and D.O. Riska, Phys. Rev. C **52**, 2925 (1995).
 - [22] S. Hirenzaki, E. Oset, and P. Fernández de Cordoba, Phys. Lett. B **378**, 29 (1996); Phys. Rev. C **53**, 277 (1996).
 - [23] L. Alvarez-Ruso, Phys. Lett. B **452**, 207 (1999).
 - [24] B.A. Li, C.M. Ko, and G.Q. Li, Phys. Rev. C **50**, 2675 (1994).

- [25] S. Huber and J. Aichelin, Nucl. Phys. **A573**, 587 (1994).
- [26] T. Hamada and J.D. Johnston, Nucl. Phys. **34**, 382 (1962).
- [27] R.V. Reid, Ann. Phys. (N.Y.) **50**, 411 (1968).
- [28] E. Rost, Nucl. Phys. **A249**, 510 (1975).
- [29] H. Arenhövel, M. Danos, and H.T. Williams, Nucl. Phys. **A162**, 12 (1971).
- [30] H. Garcilazo and E. Moya de Guerra, Nucl. Phys. **A562**, 521 (1993).
- [31] B. Juliá-Díaz, F. Fernández, P. González, and A. Valcarce, Phys. Rev. C **63**, 024006 (2001).
- [32] K. Shimizu, Rep. Prog. Phys. **52**, 1 (1989).
- [33] A. de Rújula, H. Georgi, and S.L. Glashow, Phys. Rev. D **12**, 147 (1975).
- [34] H. Garcilazo, A. Valcarce, and F. Fernández, Phys. Rev. C **64**, 058201 (2001).
- [35] H. Garcilazo, A. Valcarce, and F. Fernández, Phys. Rev. C **60**, 044002 (1999); B. Juliá-Díaz, F. Fernández, A. Valcarce, and J. Haidenbauer, in *Mesons and Light Nuclei*, edited by J. Adam, P. Bydžovský, and J. Mareš (American Institute of Physics, New York, 2001), p. 267.
- [36] K. Holinde, Nucl. Phys. **A415**, 477 (1984).
- [37] D.O. Riska and G.E. Brown, Nucl. Phys. **A679**, 577 (2001).
- [38] M. Soyeur, Nucl. Phys. **A671**, 532 (2000).
- [39] B. Juliá-Díaz, A. Valcarce, P. González, and F. Fernández (in preparation).
- [40] B. Juliá-Díaz, J. Haidenbauer, A. Valcarce, and F. Fernández, Phys. Rev. C **65**, 034001 (2002).